

Project Report on

# **Design and Optimization of Paper Bags**

Submitted in the partial fulfilment of the requirement for the award  
of degree of

**Bachelors of Technology**  
in  
**Metallurgical and Materials Engineering**



Under the guidance of

Prof. B. B. Verma

Prof. P. K. Ray

Dept. of Metallurgical & Materials Engg

Dept. of Mechanical Engg

By:

Nagadamudi Srihari  
110MM0588

Vishnu Kunchur  
110MM0589

Department of Metallurgical and Materials Engineering

National Institute of Technology, Rourkela



## Certificate

This is to certify that the thesis entitles “**Design and optimization of paper bags**” being submitted by Nagadamudi Srihari (110MM0588) and Vishnu Kunchur (110MM0589) for the partial fulfilment of the requirement of Bachelors of Technology degree in Metallurgical and Materials Engineering and is a bonafide thesis work done by them under my supervision during the academic year of 2013-14, in the Department of Metallurgical and Materials Engineering, National Institute of Technology; Rourkela.

The results presented in this thesis have not been submitted elsewhere for the award of any other degree or diploma.

Date:

Prof. B. B. Verma  
Department of Metallurgical and Materials Engineering  
NIT, Rourkela

## **Acknowledgements**

We extend our heartfelt gratitude firstly, to our mentors; Prof. B. B. Verma (Department of Metallurgical and Materials Engineering) and Prof. P. K. Ray (Department of Mechanical Engineering) for their constant guidance and motivation.

To Prof. B. C. Ray, the HOD, Department of Metallurgical and Materials Engineering

To Mr. Hembram for offering his technical expertise.

To Paul Wawrzynek and Louis Martha from the Cornell Fracture Mechanics Group for having developed CASCA and FRANC2D/L

**This body of work is dedicated to all the environmentalists of the world, fighting for the noble cause of safeguarding our planet.**

## Contents

|  |    |
|--|----|
| Abstract   | 6  |
| <br><b>Chapter 1:</b>  |    |
| Introduction   | 7  |
| <br><b>Chapter 2:</b>  |    |
| Literature Review  |    |
| 2.1: Fabrication of Jute-reinforced paper<br>laminated composite | 9  |
| 2.2: Finite Elemental Method                                     | 10 |
| 2.3: CASCA   | 11 |
| 2.4: FRANC2D/L   | 14 |
| <br><b>Chapter 3:</b>  |    |
| Simulations and Results  |    |
| 3.1: Preliminaries   | 18 |
| 3.2: Plain Bag Matrix Simulation                                 | 19 |
| 3.3: Parallel Strip Bag Model                                    | 20 |
| 3.4: Up-Down Taper Strip Model                                   | 21 |
| 3.5: Down-Up Taper Strip Model                                   | 21 |

|                                   |    |
|-----------------------------------|----|
| 3.6: Triangular Strip Model       | 22 |
| 3.7: Optimization of Strip Height | 23 |
| 3.8: Addition of Stiffener        | 27 |
| Discussion                        | 32 |
| Conclusions                       | 34 |
| References                        | 35 |

## **Abstract**

The detrimental effects of plastic bags on the environment are well known. It is now appropriate to use alternative materials for manufacturing bags and in packaging industries. While biodegradable plastics research has gained steam in the first world countries, countries like India are still dependent upon cheaper alternatives such as kraft paper/ old newspaper (ONP) as packaging materials for transport. However the lacunae associated with the employment of paper bags stem from their poor mechanical properties which make them unsuitable for use as such. The fabrication of jute-fibre reinforced paper laminates has proven to be a promising alternative to plastic bags. The current body of work is pertinent to the design and optimisation of paper bags by employing software using the Finite Elemental Analysis code developed by researchers in the Cornell Fracture Group, namely CASCA and FRANC2D. An optimal model was selected by running simulations using area of reinforcement, geometry and height of strip as variables. Simulations were initially run using steel as the material, with the mechanical properties later being changed to that of kraft paper in subsequent models. With the application of height optimized triangular strips, a reduction in peak stress of about 154KPa was observed. Effective design and optimization lead to a percentage reduction in peak stress by about 77.78%.

# Chapter 1

## Introduction

The hazards associated with the usage of single-use plastic bags, which are often distributed (for no additional cost) along with purchases in a local grocery store, for instance; are well known. Being a strong, cost-effective, hygienic and overall efficient method of transporting articles; such lightweight plastic bags have come into acceptance and use since the early 1980s in India – substituting their modest paper bag predecessors.

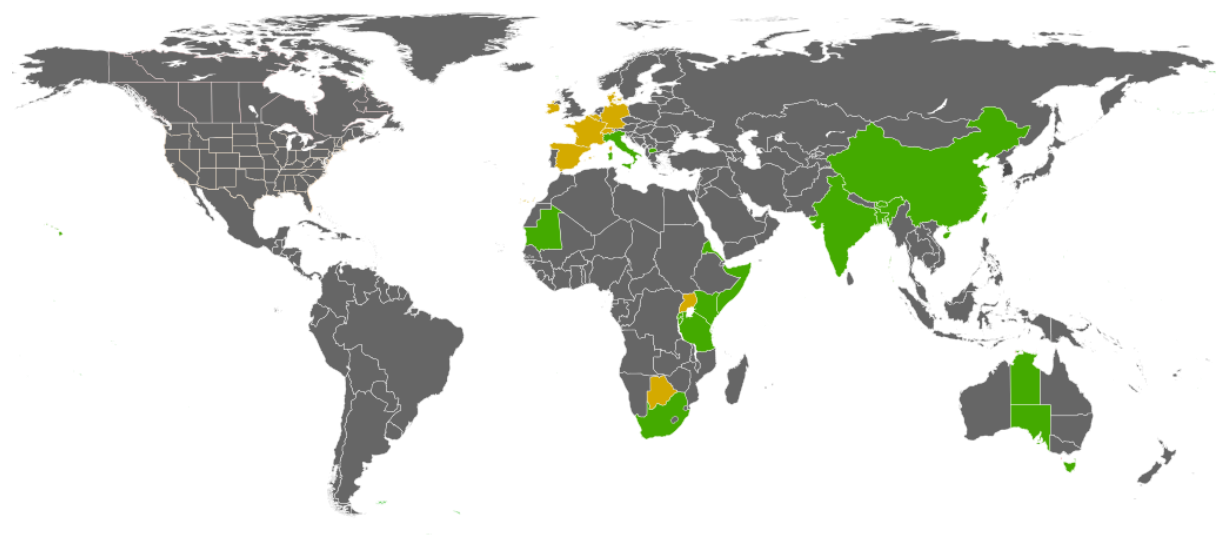


Fig1: Phase out of plastic bags across the world. The green portions indicate countries which have banned the consumption of plastic bags, while the portions in yellow indicate countries which have levied taxes on plastic bag usage.

Predominantly fabricated from high-density polyethylene (HDPE), the employment of plastic bags poses some serious problems on the frontiers of consumption of non-renewable sources (crude oil, gas, petrol etc.), disposal and overall environmental impact. According to an estimate by the World Wide Fund for Nature, the consumption of plastic bags has jeopardized aquatic life; with about 100,000 whales, seals and turtles perishing globally every year. Yet another estimate suggests that the ingestion of plastic bags, leading to the clogging of their digestive systems causes the deaths of upto 20 cows every day in India. The blockage of drains and sewer systems, the geographical issues associated with mass-scale plastic bag dumping, the non-biodegradability of HDPE plastic bags resulting in the release of several toxic substances into the environment has ensued in the coinage of a relatively new term associated with the environmental implications of discarded plastic bags: *white pollution*.

To combat the detrimental effects of plastic bag usage, the Indian government in 2002 banned the production of plastic bags below thicknesses of 20  $\mu\text{m}$  to prevent clogging of municipal drainage systems, among the many other conundrums. However, even as enforcement of the law continues to remain a problem; alternatives for plastic bags have been brought to the fore. While biodegradable plastic has proven to be a viable alternative in most first world countries, their high costs limit their usage in third world countries such as India. One of the major alternatives as a solution to the problems posed by plastic bag usage in India has manifested in a resurgence in the employment of traditional paper bags. Ranging from local grocery shops to branded stores in supermarkets, a reversal trend has been observed, with a steady increase in the usage of paper bags. Bleached/unbleached kraft paper and old newspaper can be employed as packaging material for transportation of goods. However, paper bags have their own demerits. The aforementioned attributes of plastic bags are largely absent in paper bags, with ease of transportation, flexibility and bag strength being concerns. The major problem though, stems from the poor mechanical properties of paper including low strength and tear resistance.

In order to improve the poor mechanical properties of paper such that the factors linked to incompetence as viable packaging material may be mitigated, Verma et al [2007] fabricated a continuous jute-fibre reinforced laminated paper composite. The mechanical properties of the composite material were observed to be superior to those of plain paper. Jute reinforced paper composites were thus established as a viable material for fabricating paper-based bags. However, it becomes important to design and optimize these laminated paper-composite bags in order to obtain an optimal stress distribution, minimize peak stresses to delay failure and optimum utilization such that greater loads may be borne by the paper bags for longer periods of time. The current body of work is an undertaking of the same.



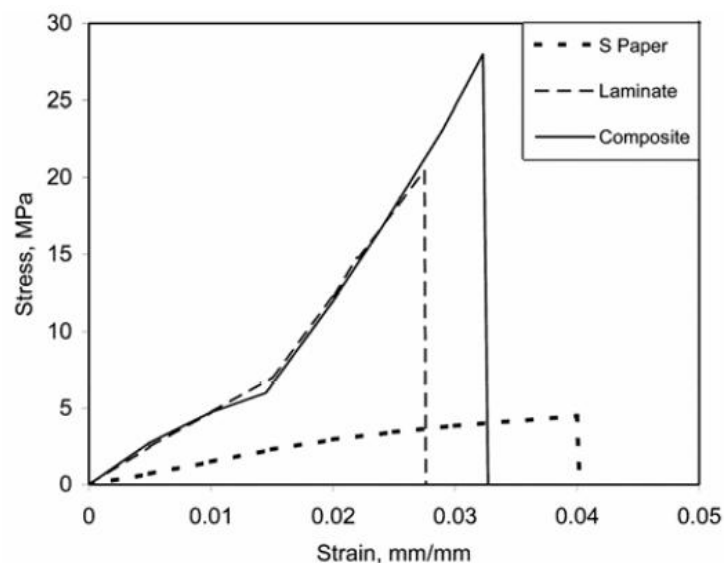
## Chapter 2

### Literature Review

#### 2.1: Fabrication of jute-reinforced paper laminated composite:

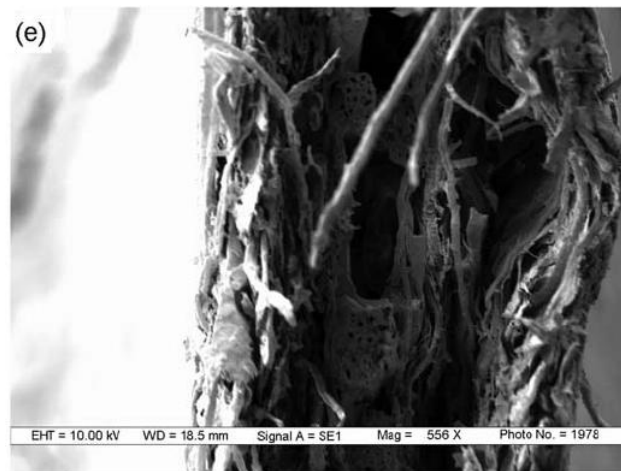
As a viable alternative to plastic bags, a new paper-based material was developed to impart higher strength and tear resistance to paper. A jute reinforced laminated paper composite was fabricated by reinforcing different types of kraft paper and old newspaper (ONP) with jute fibre of average diameter 0.045mm and tensile strength 470 MPa. White corn flour based glue was freshly prepared for usage as an adhesive to enable adherence in the paper matrix. A pair of paper strips were taken to fabricate the fibre reinforced laminated paper composite. On the coarser surface of one of the strips (about 120mmx25mm) a thin layer of glue was applied evenly. Batches of 0.02-0.08g of jute fibres which were evenly separated were laid upon the glued surface parallel to the length of the paper strip. Another paper strip was carefully glued and stuck to the former paper strip (with the jute fibres glued to it). In order to remove excessive adhesive, trapped air pockets and enhance adhesion between matrix and reinforcement, the jutepaper sandwich was successively rolled. Bending and uneven corrugation was avoided by placing the composite between two glass slabs. Oven drying at 60°C was performed thereafter.

The fibre reinforced composites were subjected to mechanical and optical characterization. Tensile specimens were created by making tumbler shaped specimens for mechanical testing, to avoid slipping/fracture while gripping from the jaws. A comparison between the tensile strengths of paper, laminated paper and laminated paper composite is presented below:



Clearly from the plot above, we may infer that there is a considerable increase in tensile stress while using laminated paper as when compared to a plain sheet of kraft paper. The decrement in ductility is commensurate with a marked improvement in tensile strength by almost 600%. When reinforced with jute, the composite displays a further increase in tensile

strength of almost 8 MPa, along with a slight increase in ductility. Displayed below is a fractograph of the jute reinforced laminated composite:



Fractograph of 0.05gm fibre-kraft paper composite

From the fractograph it is apparent that glue starved pockets and shorn fibres are present. The capillary action of jute fibres may have lead to a loss in sufficient adhesive to bond the fibre-matrix interface. The effect of interfaces on the fiber-matrix bonding also plays a major role. In summary, laminated paper exhibits a manifold increase in mechanical properties (tensile strength) as when compared to plain kraft paper/ONP. A substantial increment in load bearing capacity, tensile strength and fracture energy is observed in case of fibre reinforced paper laminated composites, which establishes the material as a potent packaging material and a formidable alternative to plastic bags.

## 2.2: Finite Elemental Method:

A numerical technique for finding the approximate solutions to boundary value problems, the Finite Elemental Method is particularly useful in designing structures. Variational methods are employed to minimize error functions, leading to a stable solution. It is in essence an integrative method where several tiny elements are used to construct a larger entity. There are several advantages associated with the subdivision of a domain into smaller units:

- A complex geometry may be accurately represented
- Dissimilar material properties may be included
- The total solution may be easily represented.
- A good insight to the local effects may be observed

A typical solution to a problem via the FEM route involves (1) Division of the entire matrix into several subdomains, with each of these subdomains being governed by a particular equation (2) recombining the individual elements systematically so as to arrive upon the final solution to the problem at large.

Step 1: To locally approximate the complex equations that govern the body as a whole, the elemental equations are determined. The original equation is often a partial differential

equation. The FEM is often described as the typical case of the Galerkin method in order to explain the approximation in the process. The integral of the residual and weight functions is constructed, with the integral being set to zero in this technique. The errors of approximation are minimized by the fitting of trial functions into the partial differential equations. What remains is the error caused by the trial functions, with the weight functions being polynomial approximations which project the residual. All spatial derivatives are eliminated from the PDE, resulting in a local approximation of the PDE with

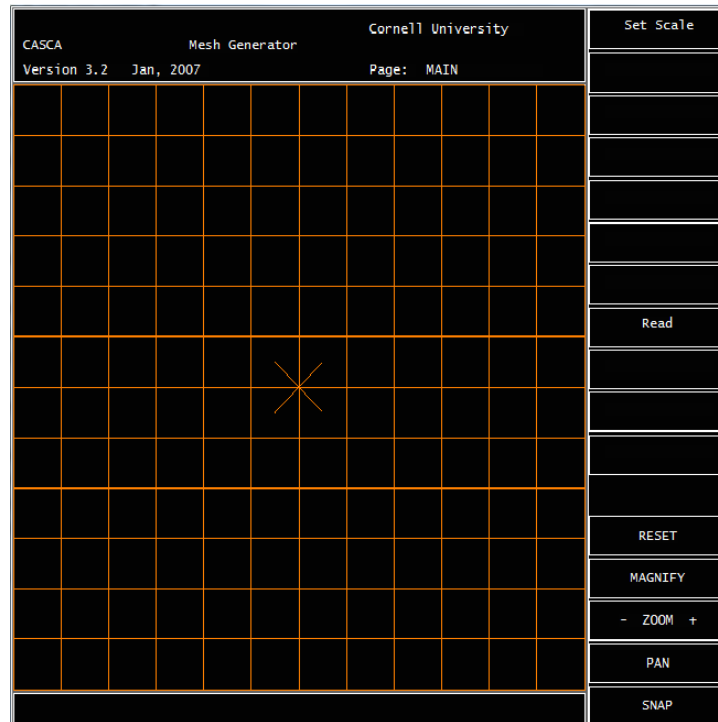
- a set of algebraic equations for steady state problems,
- a set of ordinary differential equations for transient problems.

Step 2: The equation sets thus, basically denote the element equations. Numerical methods in linear algebra are used to solve the problems, using standard techniques such as Euler's method or Runge-Kutta's method. The local subdomain nodes have their coordinates transformed to the global scale by the generation of element equations. FEM software uses coordinate data generated from subdomains to solve the problem globally.

The practical application of FEM is finite elemental analysis (FEA), which becomes a particularly useful tool for engineers, since it serves as a computational method for performing engineering analysis. FEA involves the generation of a mesh for dividing the complex problem into several smaller elements, which is often coupled with a software program embedded with the FEM algorithm. Since FEA can be employed over a wide range of problems encompassing structural, thermal and electromagnetic fields, several software have been developed over the years to cater to the requirements of engineers. In order to analyse and solve structural problems, the Cornell Fracture Group invented and distributed a free FEA software, namely FRANC2D. FRANC2D bears the FEA code required for the requisite analysis, however; in order to execute FRANC2D, a preprocessing mesh creator is required to build the structure for failure analysis. In order to design and optimize laminated paper bags, computer based simulations via FEA were required to be conducted for which CASCA, a mesh-creation software was used as a pre-processor to FRANC2D, in lieu of facilitating analysis. Since the simulation involved the usage of multiple layers, FRANC2D/L was used instead of FRANC2D.

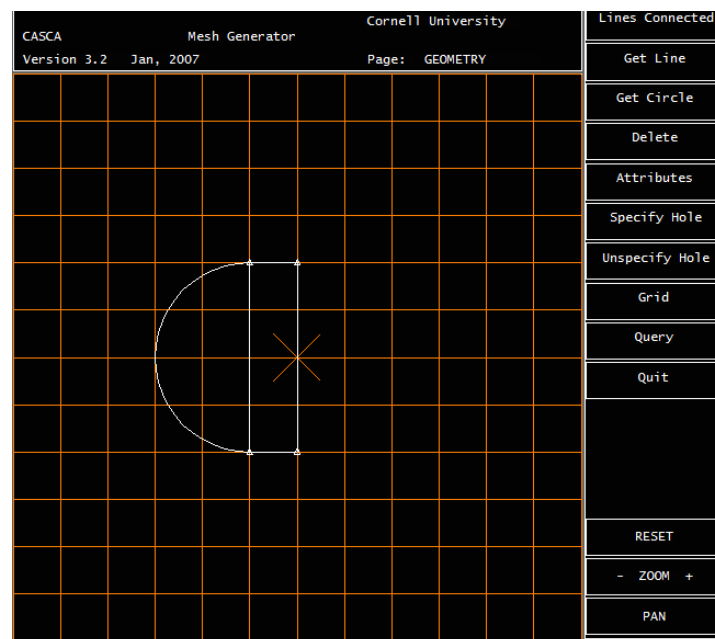
### 2.3: CASCA:

CASCA is an interactive program for the creation of two-dimensional continuum finite element meshes. CASCA was originally developed by Paul Wawrzynek and Louis Martha at the Cornell University as a test bed for a hierarchical data base that was later implemented in FRANC3D. However, it has proven to be a useful tool, and has continued to live beyond its initial application. The process of building a mesh using CASCA for further FEA is initiated by the creation of a boundary confining the area being subjected to analysis. Further subdivision of the domain into elements is performed, effectively creating a mesh. Only a subset of the total usable functions in CASCA are required to perform the simulation, and the procedure adopted is specified as follows:



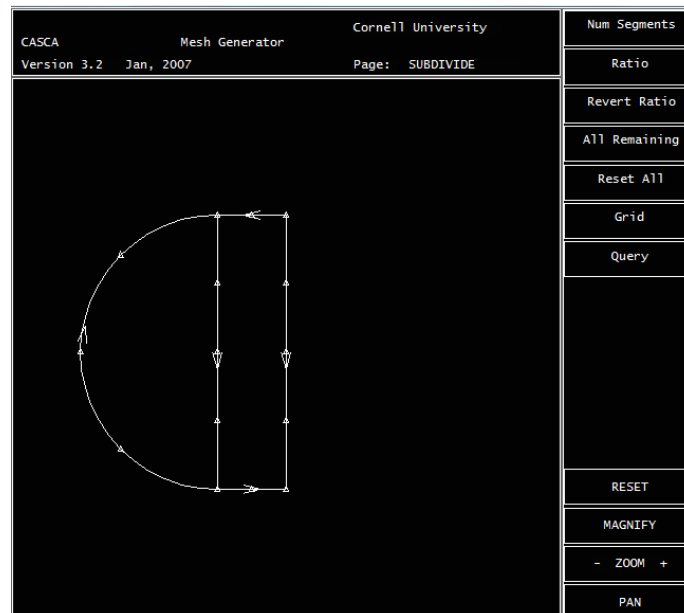
Snapshot of the CASCA workspace

- 1) Setting scale: The workspace coordinates may be changed according to the users' convenience. The default scale setting is 12x12 with the centre of the grid being  $(X,Y) = (0,0)$ .
- 2) Geometry: Using an assortment of lines and arcs, the required domain is created. Once the outline of the domain is created, internal sections may be generated by using the SUB REGIONS option.



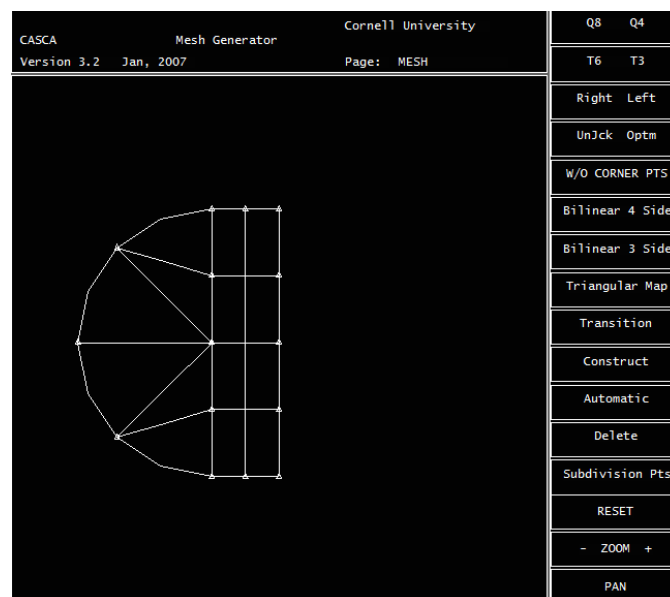
Outline of the domain

3) Sub Divisions: One specifies nodal densities for FEA analysis via the SUB DIVISIONS segment. The orientation is indicated by the direction of the arrow and is used for varying density along the edges. In this particular case, a nodal density of 4 has been specified along the vertical lines and arc, while a nodal density of 2 is specified along the breadth of the rectangular region.



Nodal densities specified along all edges

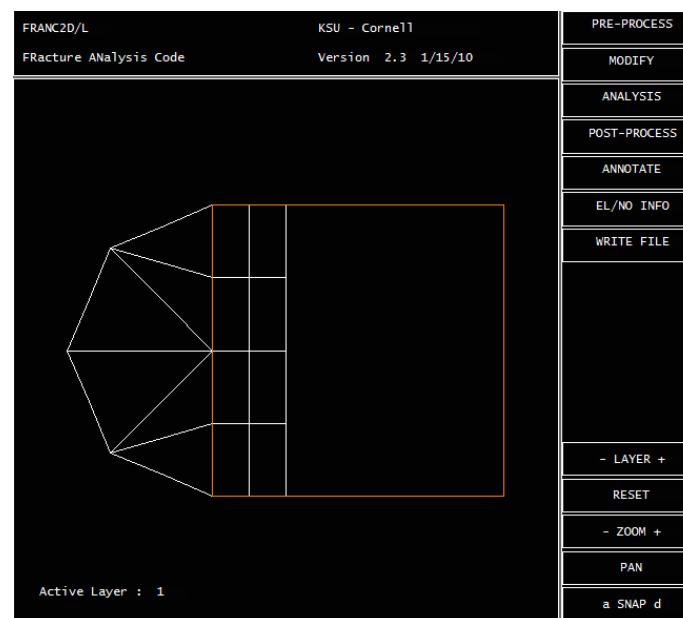
4) Creating a mesh: The default elements in CASCA are the Q8 quadrilateral elements and the T6 triangular elements. BILINEAR 4SIDE and BILINEAR 3SIDE are useful for meshing quadrilateral and triangular regions respectively, however it must be noted that in case of quadrilateral meshing the nodal densities on opposing sides must be the same. In simple mesh constructions, the AUTOMATIC option may also be used.



The CASCA workfile may thereafter be saved in the .csc format, or may be saved directly for FRANC2D simulation in the .wdb format. The current problem however, employs multiple layers (as mentioned earlier) and hence it becomes important to use a **castofranc** generator file which functions by riveting two overlapping meshes. For this purpose, another mesh is generated, overlapped as a second layer and exported as a FRANC2D/L workfile.

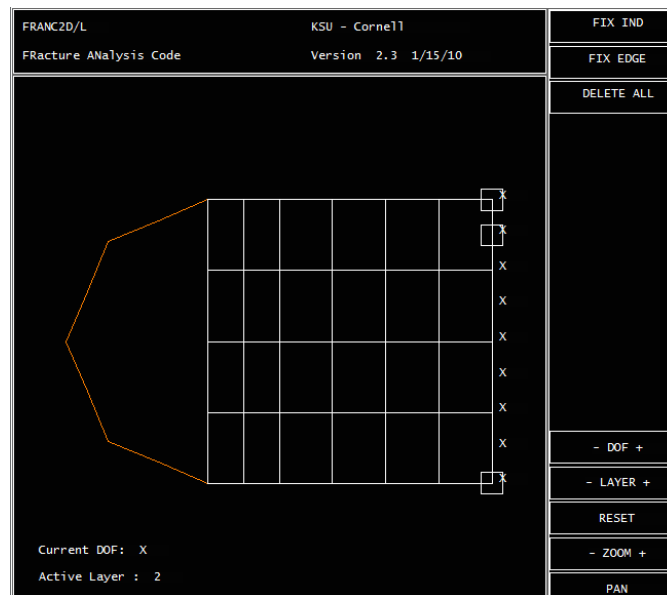
## 2.4: FRANC2D/L:

FRacture ANalysis Code in 2D was developed by the makers of CASCA as an FEA software for structural purposes. FRANC2D/L is an improvisation over the original FRANC2D software, whereby working on multiple layers is permissible. Once a compiled FRANC2D workfile has been created by merging both CASCA layers in the .inp format, the file can be opened by FRANC2D/L. The process steps are outlined (by proceeding to analyse the mesh created earlier via CASCA) as follows:



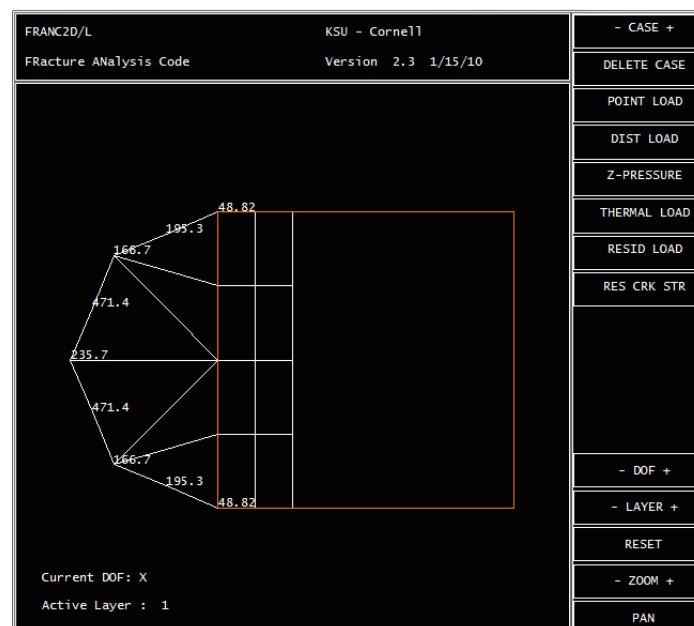
1) Pre-processing: The problem type is to be specified. By default, the simulation shall be performed in the Plane STRESS mode. The MATERIAL option is to be selected accordingly by entering appropriate values in the terminal window. The Young's Modulus (E), Poisson's Ratio ( $\nu$ ), Thickness of material (T) and Stress Intensity ( $K_{IC}$ ) values are to be entered. For the purposes of the simulations we perform, the thickness and stress intensity have no bearing and hence are maintained constant for all simulations (i.e. constant values of 1). Since an adhesive material is being used to bond the layers, a new adhesive material must be created from MATERIAL+. The shear strength and thickness values of the adhesive layer need to be entered for this purpose. The adhesive layer is displayed in the terminal window as Layer 3.

2) Boundary Conditions and Loads: The FIXITY option is used to fix an edge/point of the mesh. These selected nodes remain invariant from their original position.



FIXITY applied to second layer, immobilizing the structure along the X-axis at that point

The DIST. LOAD option lets us choose the required mode of load distribution. Load may be applied either at a node or along a line, along either axis. The applied load is compressive in nature and deforms the material owing to its fixture.



Load distributed along length of Layer 1

3) Modify: Since an adhesive layer has been used, the elements serving as adhesive elements in the overlapping mesh need to be specified. The ADD ADHESIVE -> TOGGLE ALL option selects all the elements common to the overlapping mesh of both layers. Once the adhesive elements have been selected, a DIRECT STIFF, LINEAR analysis needs to be performed under the ANALYSIS option in order to assess the effect of application of loads (and adhesive, in this case) on the domain. A Gauss Elimination method is enforced by the

code for this purpose. The terminal window displays a message indicating the back-substitution time, equation renumbering time, decomposition and assembly time as shown:

```

Reduce bandwidth:
Zero Gstf:
Assemble:
Backsubstitution:

*****
                        FRANC Analysis Report
                275   Equations                9280   Stiffness coefficients

Total Time <inc overhead> : 1193046:
Renumber equations Time   :      0:00
Bandwidth reduction Time  : -1431655
Assembly Time             : 66810602
Decomposition Time        : -2075900
Backsubstitution Time     :      0:00

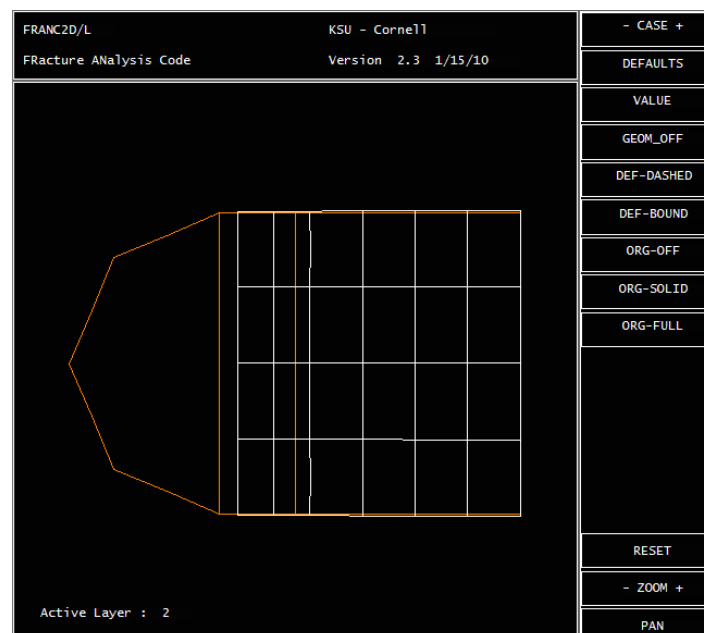
Total Work                 : 171.61

*****

Analysis done

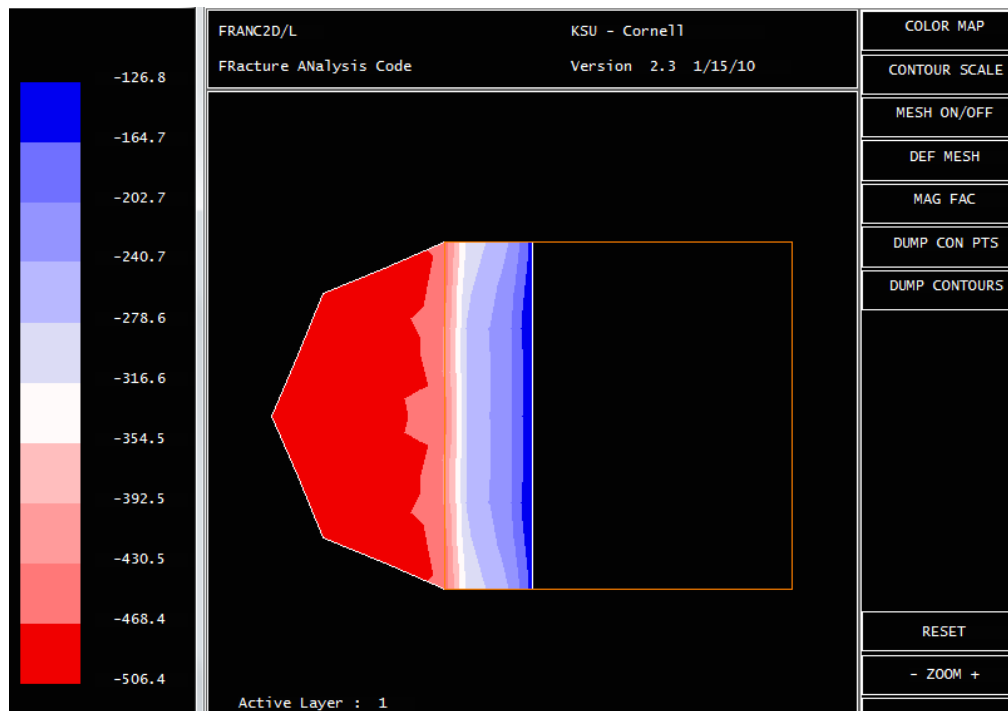
```

5) Post-processing: The post-processing option can be used only once the DIRECT STIFF analysis has been performed. Post-processing allows us to examine the deformed mesh, the contours associated with stress distribution, determine the peak stresses among many other functions. The deformed layer-2 mesh, post-processing is as follows:



The peak stress values may thereupon be estimated by assessing the contour option. In this case, since load has been applied in the X direction, the Sig  $X_{max}$  value can be determined from the plot as shown:





Owing to the compressive nature of the applied load, the contour region is predominantly red, implying maximum compression. Minimal compression is visible in the region adjoining the adhesive area.

## Chapter 3

### Simulations and Results

#### 3.1: Preliminaries:

The design and optimization of laminated paper bags was carried out exclusively via FRANC2D/L as the FEA software, employing CASCA to create the domain mesh. FRANC2D/L was used to simplify the case by considering only one side of the bag, applying loads on the bag matrix in the regions where handles would potentially be riveted. A standard shopping bag of dimensions 38x30 units was used as the baseline and optimisation by improvement of stress distribution and minimisation of peak stress values to ensure longevity of the paper bag was attempted. The simulation essentially mimicked a tensile test, with one end of the bag fixed and the load applied being distributed upon a unit length at the other end of the bag.

Owing to the relatively low tensile stress values of paper/paper composites, we observed that it became increasingly difficult to log data. Since stress distribution remains invariant with change in material (with only the stress values changing), it was decided that the simulations would be carried out using the default FRANC2D/L material, i.e. steel. At the position of the handles, a load of 500 pounds was applied (upon each handle).

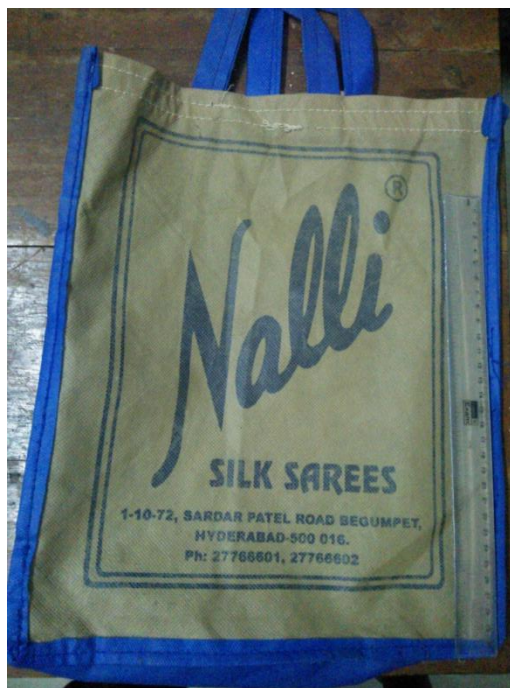
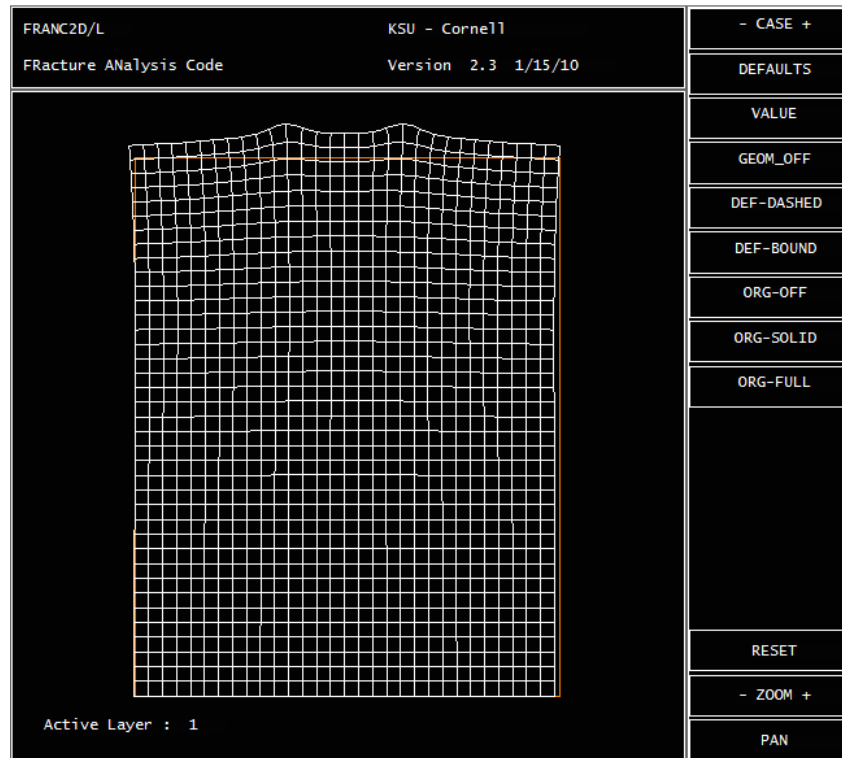


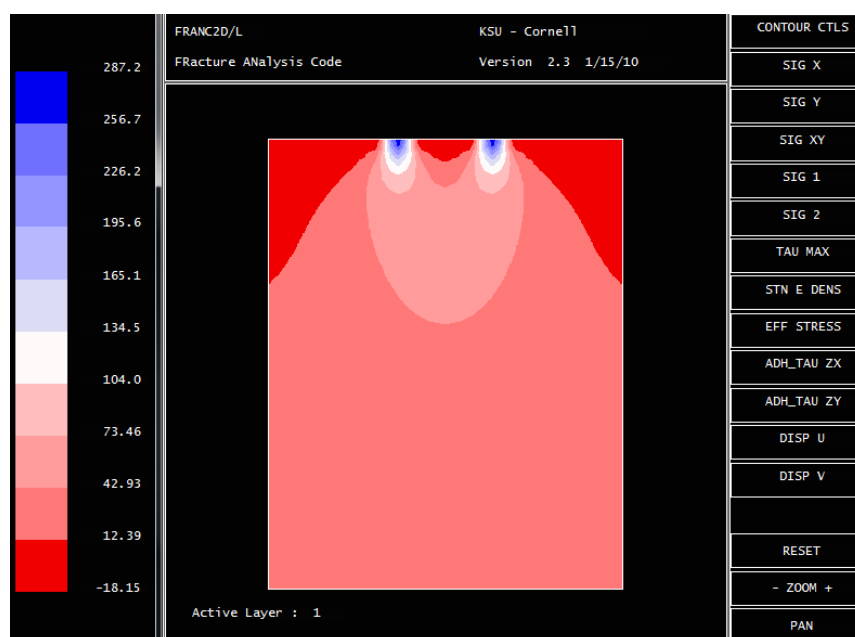
Image of the bag chosen for simulation (38cmx30cm side)

### 3.2: Plain Bag Matrix Simulation:

A model of the chosen bag was created using CASCA bearing dimensions of 38x30 inches (scaling up the bag dimensions by a factor of 2.54). The lower end of the bag was fixed by FIXITY and a fixed load of 500 pounds was applied on each handle. The deformed mesh obtained post-processing is depicted as follows:



The peak stress value and stress distribution is estimated from the Sig Y<sub>max</sub> contour plot of the bag matrix:



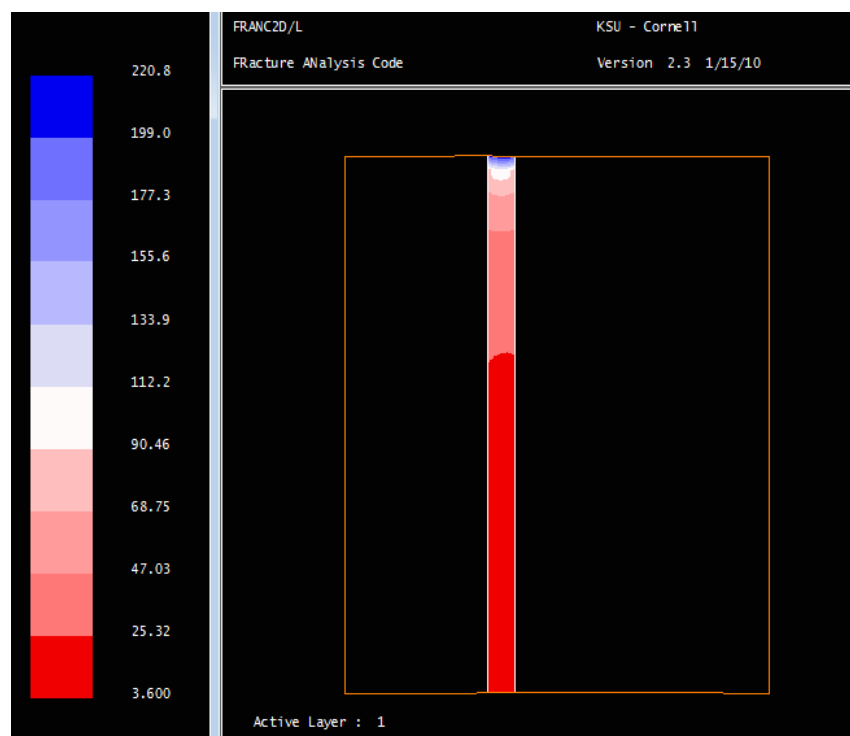
From the contour plot, it is clear that the  $\text{Sig } Y_{\max}$  value equals 287.2 psi. In accordance with intuition, the surrounding area is in a state of compression. The region under maximum stress essentially has highest propensity for failure to occur. In order to lower the peak stress value and reduce the area under maximum stress to further lower the probability of failure to occur, the adoption of “load bearing strips” was decided upon. Simulations were run by engaging parallel strips running across the entire length of the bag.

### 3.3. Parallel-Strip Bag Model:

Parallel strips of width 2inch, running across the length of the bag were created as an additional layer and superimposed upon the matrix of the bag with an adhesive material bonding the two. The shear strength and thickness of the adhesive material was maintained at  $G = 10,000\text{psi}$  and thickness = 0.005inch.

It was inferred from the plot that the peak stress value dropped to 220.8psi with the usage of a parallel strip reinforcing the matrix. Owing to symmetry of the structure, using one parallel strip mirrors the effect of using another. A decrement of 66.4psi was thus observed.

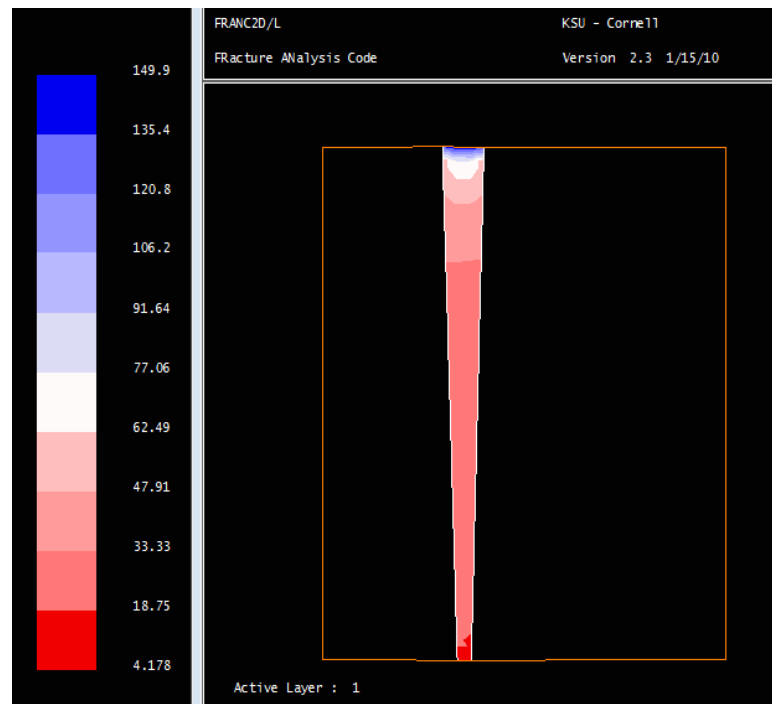
Keeping strip spacing constant, the width of the parallel strip was altered from 1 to 5 inch. A steady decrease in the  $\text{Sig } Y_{\max}$  was observed, with values dipping steadily from 439.8 to 88psi.



Contour plot for parallel-strip reinforced bag

### 3.4: Up-Down Taper Strip Model:

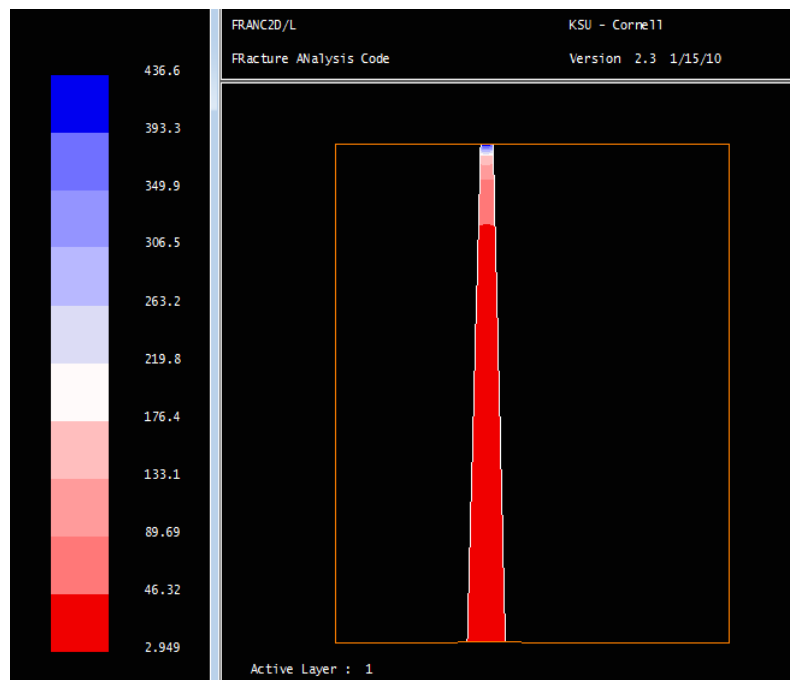
Maintaining the strip area constant at  $2 \times 38 \text{ inch} = 76 \text{ sq. inch}$ , strips of different geometries were fabricated. The creation of a trapezoidal strip was conceived by maintaining a constant strip area (equivalent to that of a 2 inch wide parallel strip). Thus, a matrix reinforced with a trapezoidal strip bearing  $3 \text{ inch} \times 1 \text{ inch}$  dimensions on opposite sides was simulated.



The  $\text{Sig } Y_{\max}$  value was observed to be 149.9 psi.

### 3.5: Down-Up Taper Strip Model:

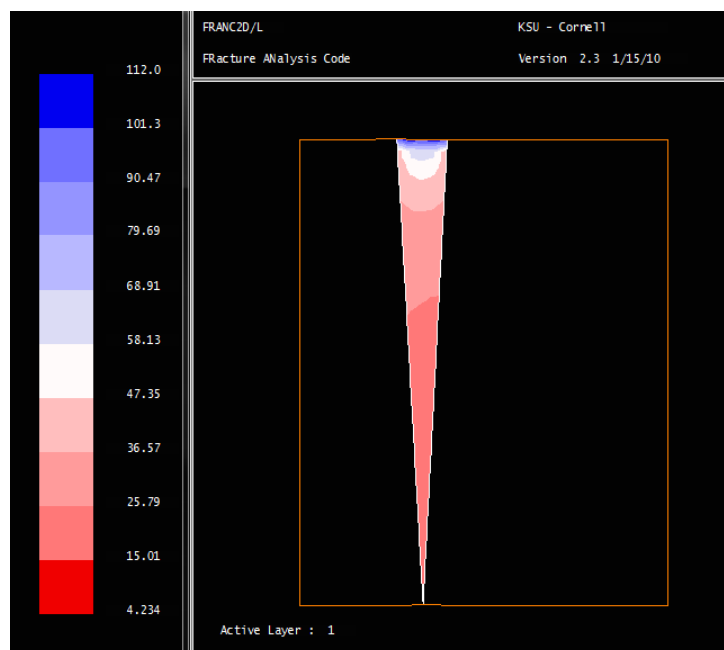
Akin to the up-down taper strip model case, with the exception that the trapezoidal strip in this case was inverted, with the load being applied upon the 1cm end; the strip area was again maintained to be the same as that in 3.3 and 3.4.



A high increase in  $\text{Sig } Y_{\max}$  value was observed, with a substantial portion of the strip being subjected to compressive forces. The  $\text{Sig } Y_{\max}$  value of the strip was observed to be 436.6 psi.

### 3.6: Triangular Strip Model:

Again, maintaining a constant value of strip area; a triangular strip was used as a load bearing reinforcement for the bag matrix. With a base width of 4 inches, an isosceles triangle strip was used across the length of the bag such that the strip area remained constant:



The peak stress value was observed to hit an overall minimum, at 112.0 psi. The global minimal value of 112.0 lead us to believe that while maintaining a constant strip area, the best stress distribution and  $\text{Sig } Y_{\max}$  value obtainable was possible by incorporating a triangular strip with load being applied at the base of the strip. For the course of further simulation and design of strip-bags, we decided to adopt up-down taper and triangular strip models in lieu of optimizing the height of the strip.

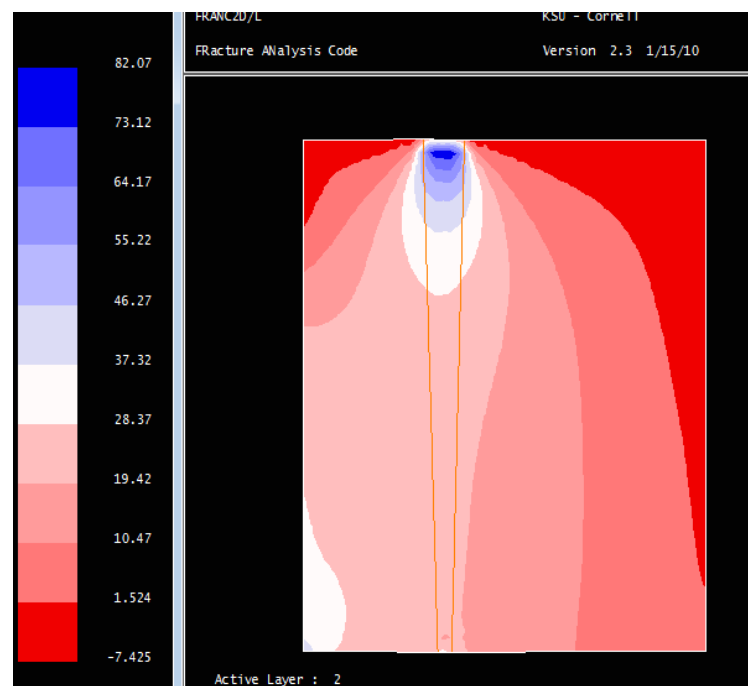
### 3.7: Optimization of Strip Height:

By maintaining a constant strip area and assessing  $\text{Sig } Y_{\max}$ , we managed to decide upon the basic families of models which could prove to be advantageous for use as reinforcements to the plain bag matrix. However, it now became important to optimize the height of the individual strips while maintaining the other dimensions of the strip, since a reduction in area would directly lead to a reduction in cost associated with manufacturing; thereby economizing the process.

#### 3.7.1: Up-Down Taper Strip Height Optimization:

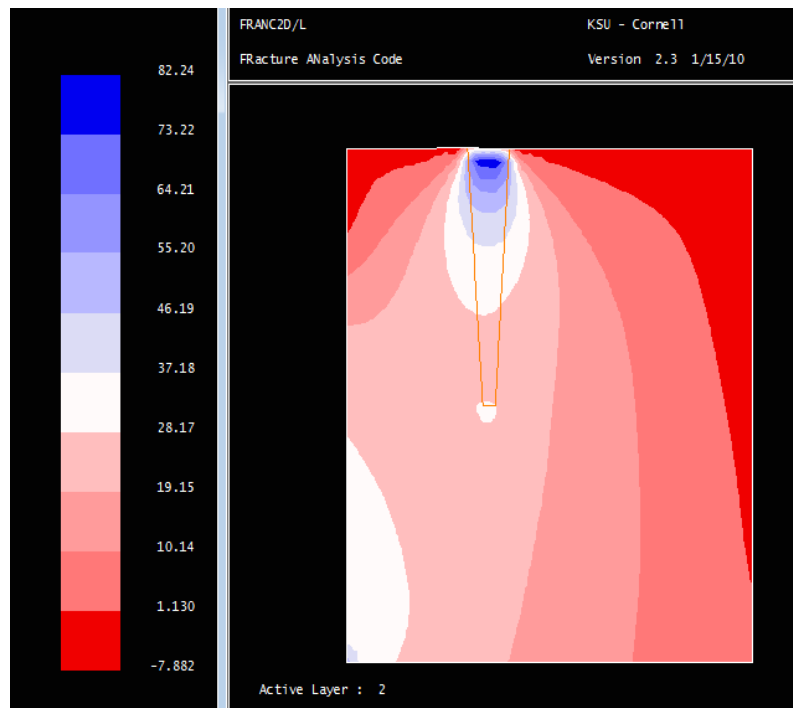
Upon loading the strip, the load essentially is transferred to the matrix of the bag, and the lesser the load that is transferred to the matrix, the better the design, since the load-bearing capacity of the strip is comparatively much better. The central idea was to reduce the height and observe the effects of strip-height reduction on stress distribution upon the bag matrix.

At full length of the height of the bag, the stress distribution produced by the up-down taper strip is as follows:



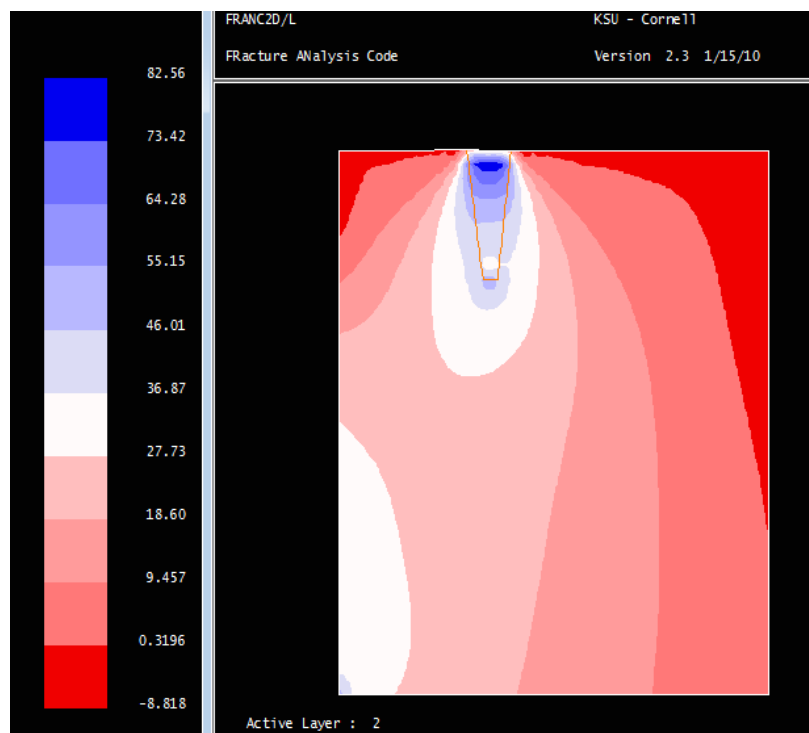
$\text{Sig } Y_{\max}$  on bag matrix = 82.07psi

At strip length equalling half the length of the bag, the stress distribution obtained for the bag matrix is:



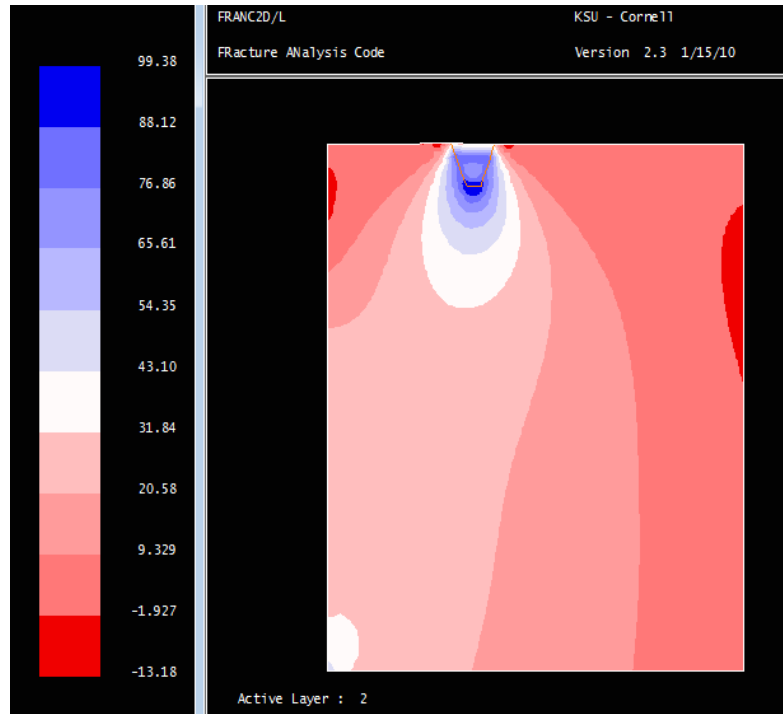
$$\text{Sig } Y_{\max} = 82.24 \text{ psi}$$

With a negligible variation in peak stress, we observe that even a reduction of stress area in half has little bearing upon the peak stress value. We further decided to reduce the height of the strip by running a simulation with strip length equal to a quarter of the bag length:

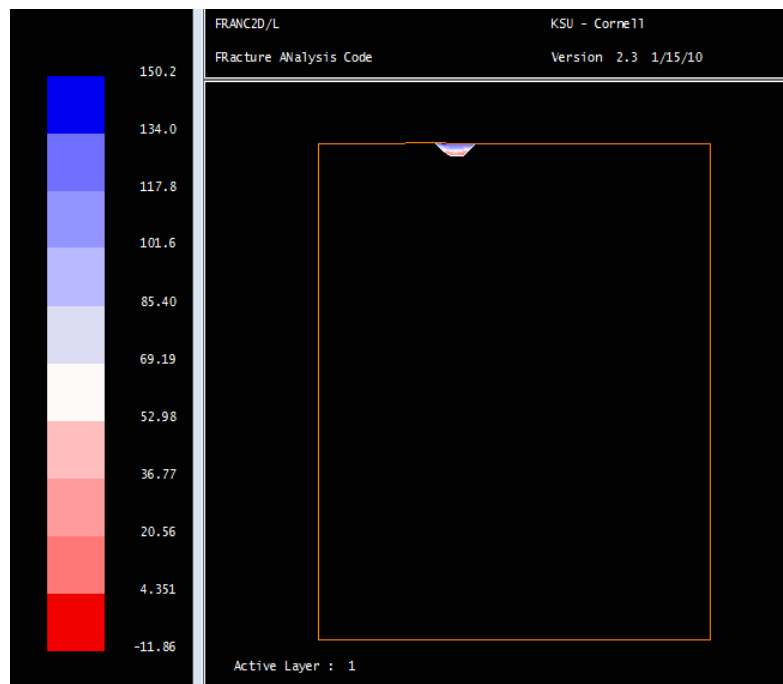




Again, we observe no difference in the peak stress value, implying that even a strip length equal to a quarter of the bag length would produce the same kind of peak stress as that of a full-length strip. Two cases were looked into: with strip height equal to 3 inches and strip height equal to 1 inch:

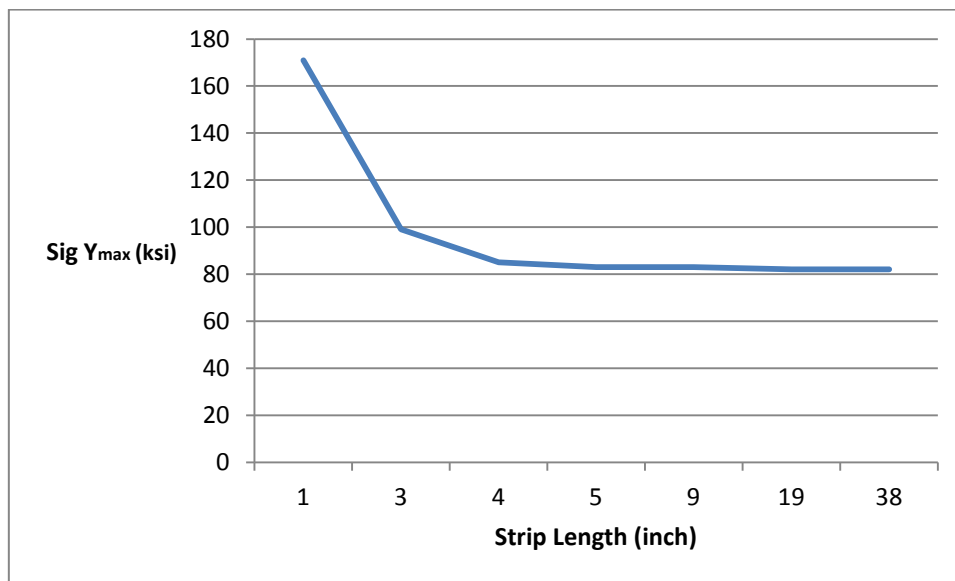


Strip height = 3inch, Sig  $\sigma_{max}$  = 99.38 psi



Strip Height = 1 inch, Sig  $\sigma_{max}$  = 150.2 psi

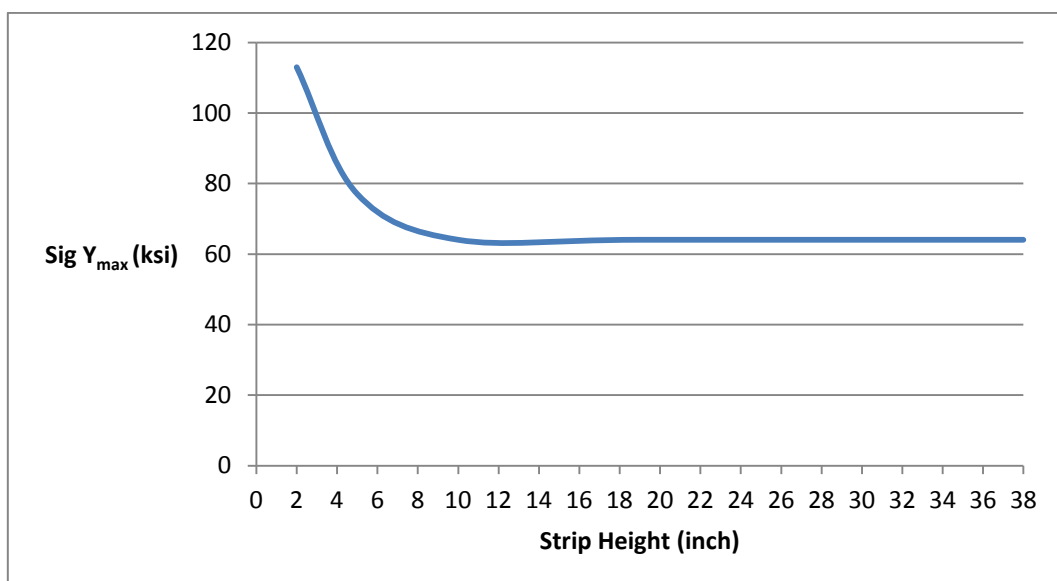
Clearly from the contour plots above, when the height is lowered below a quarter of the full length, the peak value of stress increases drastically. A plot of strip height vs. peak stress for the up-down taper model (with other dimensions remaining constant) is presented below:



Clearly from the plot, peak stress value remains constant beyond a strip height of 4 inches, and hence in lieu of optimizing strip area, full length strips need not be used, with partial strips having a height of  $h/4$  (with  $h$  being the total length of the bag) sufficing.

### 3.7.2: Triangular Strip Height Optimization:

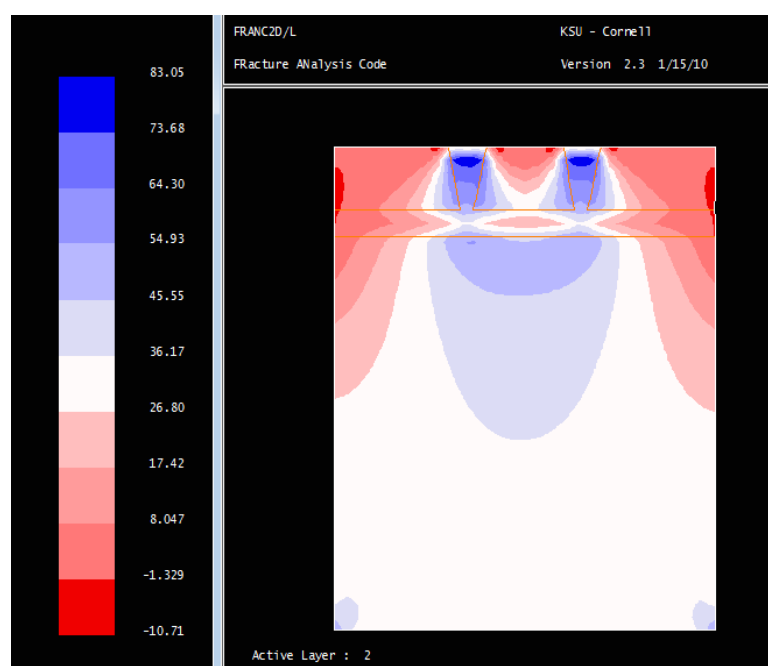
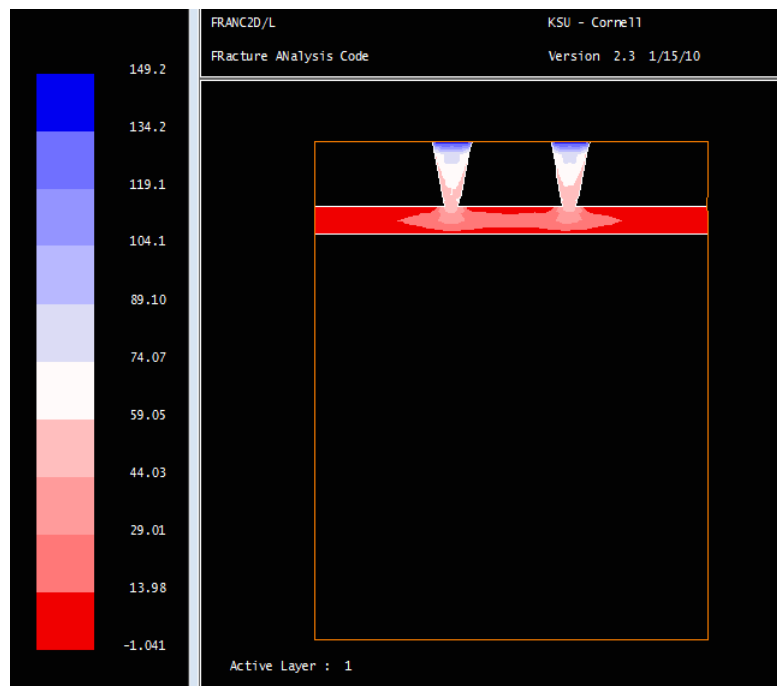
As established in case of the up-down taper trapezoidal strips, full length strips are unnecessary and in order to economize the process, partial strips may be used. Simulations were run for bag matrices being reinforced with triangular strips of varying heights, and the following plot was obtained:



Upon comparison, it is clear that the peak stress values are lower in case of triangular strips (constant  $\text{Sig } Y_{\max}$  with strip length greater than  $h/4$  being 63 psi). Hence, both up-down taper and triangular strips with a strip length close to  $h/4$  seem to be viable contenders for bag matrix reinforcements.

### 3.8: Addition of Stiffener:

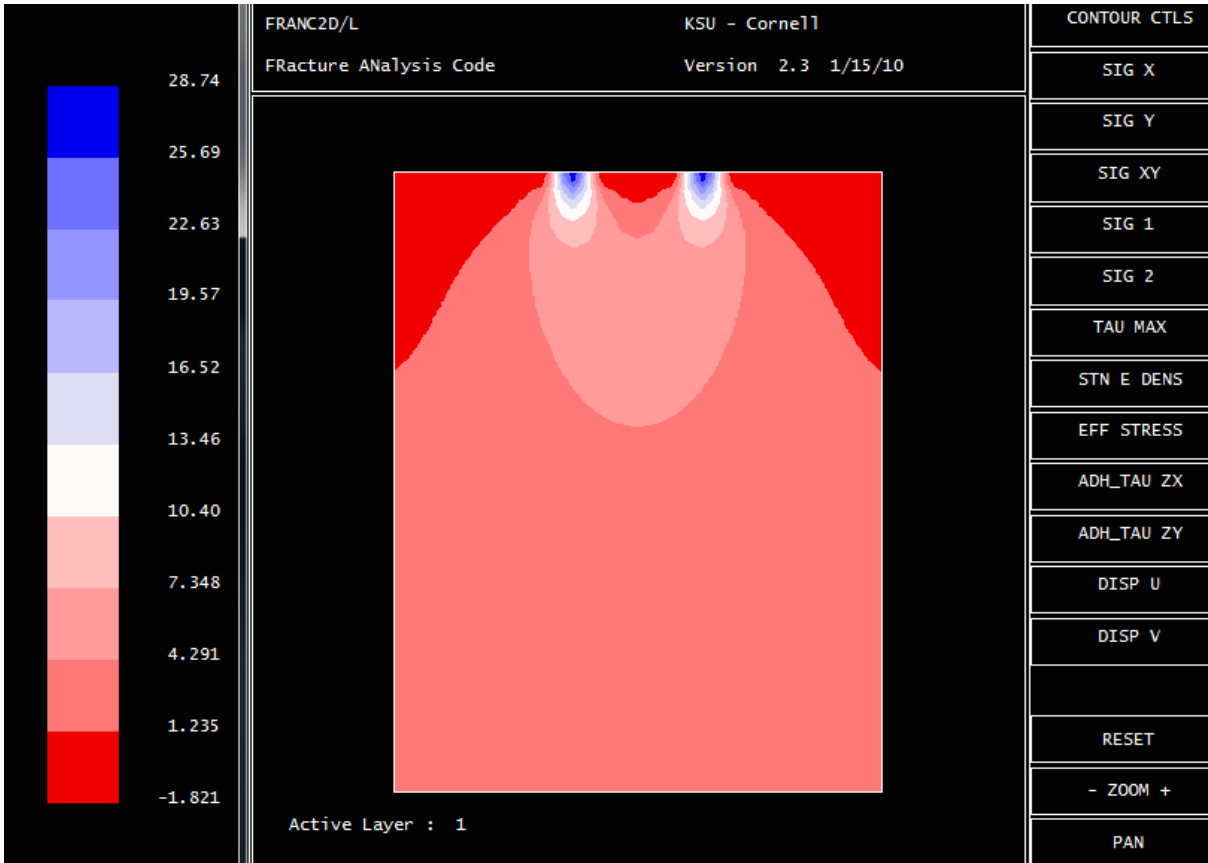
The addition of a central reinforcement to evaluate the effect on peak stress value was carried out for a height-optimised up-down taper strip:



When referenced with the peak stress vs. strip height plot for the trapezoidal strips, we observe that there is hardly any difference in peak stress values on either layer (i.e. strip or matrix) and thus concluded that the presence or absence of a stiffener does not have a substantial impact upon the peak stress value of the model.

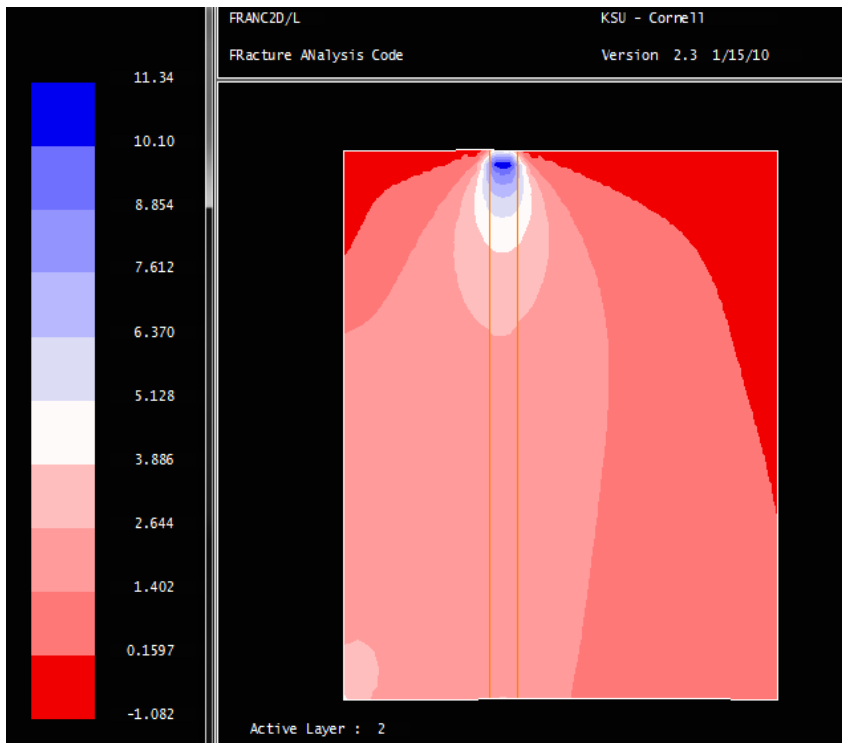
### 3.9: Simulation employing mechanical properties of paper:

The viscoelastic properties of paper have been recognized by scientists as early as the early 1960s. The viscoelastic properties of paper were studied by Brezinski using tensile-creep tests. It is a well known fact that paper is an anisotropic material. However, from the literature reviewed, isotropic properties were assumed under certain constraints. For the purposes of our simulation, the Young’s modulus and Poisson’s ratio were determined from the standard formulae prescribed for estimating the mechanical properties of paper from literature, owing to the huge variance in varieties of paper. For kraft paper of thickness 0.03 inch, the Poissons ratio is mentioned to be 0.308. The elastic modulus of kraft paper was noted to be 798psi. To check compliance with the steel based simulations, the same models were simulated. The results obtained are presented below:



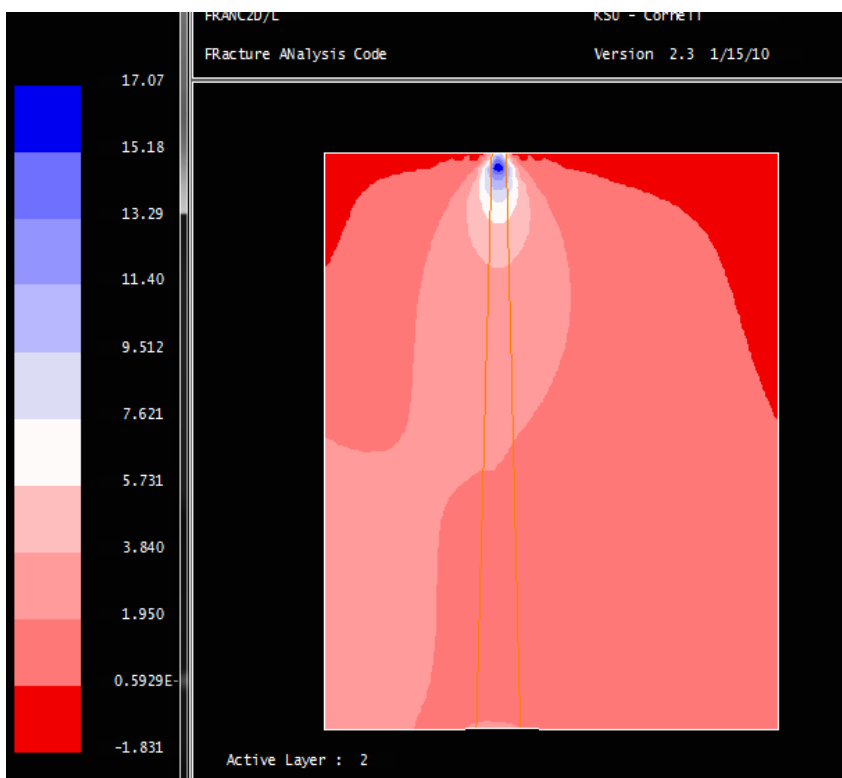
Plain Bag matrix, analyzed with kraft paper as matrix material, psi = 28.74psi

The parallel strip model, taper strip and triangular strip models are presented as follows:



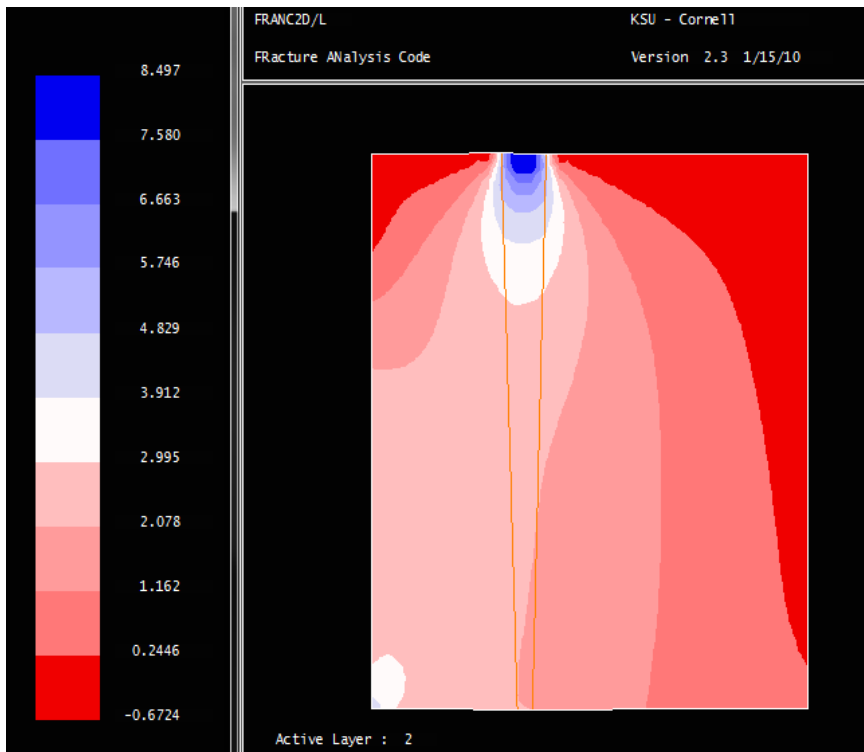
Parallel strip reinforcement

$$\text{SigY}_{\max} = 11.34\text{psi}$$



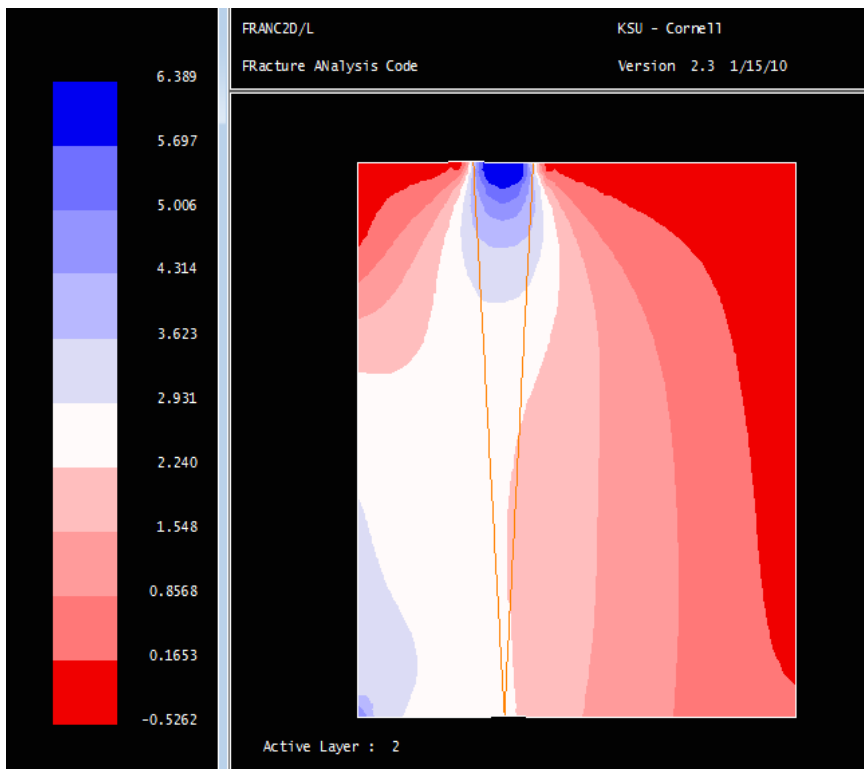
Down-up taper strip

$$\text{SigY}_{\max} = 17.07\text{psi}$$



Up-down taper

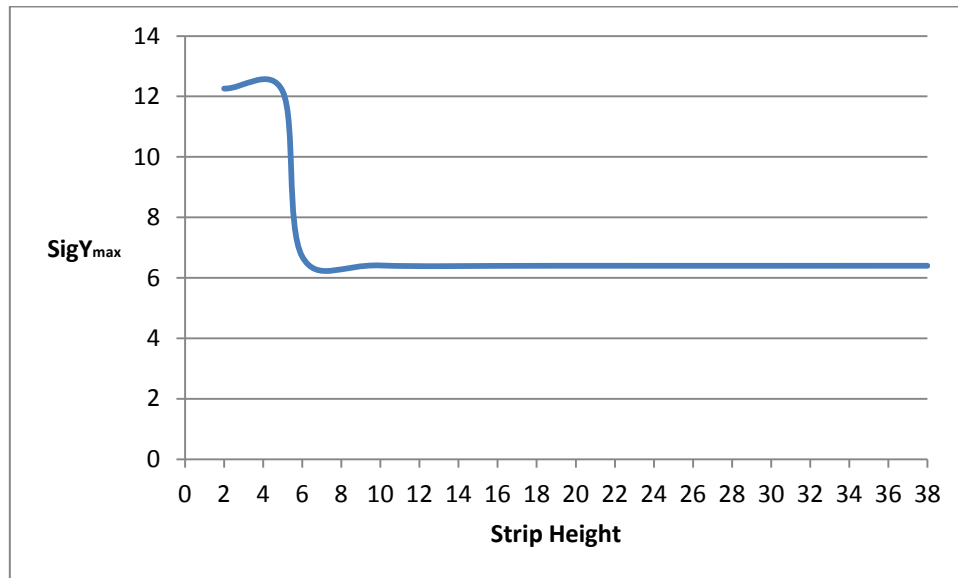
$$\text{SigY}_{\text{max}} = 8.497\text{psi}$$



Triangular strip

$$\text{SigY}_{\text{max}} = 6.389\text{psi}$$

Clearly, from the contour plots it is inferred yet again that triangular strips yield best stress distribution and least peak stress. An attempt was made to optimize the height in order to determine optimal strip dimensions for the triangular strip. Triangular strip models comprised of strip heights ranging from 2inches to 38inches were simulated. The plot obtained is illustrated below:

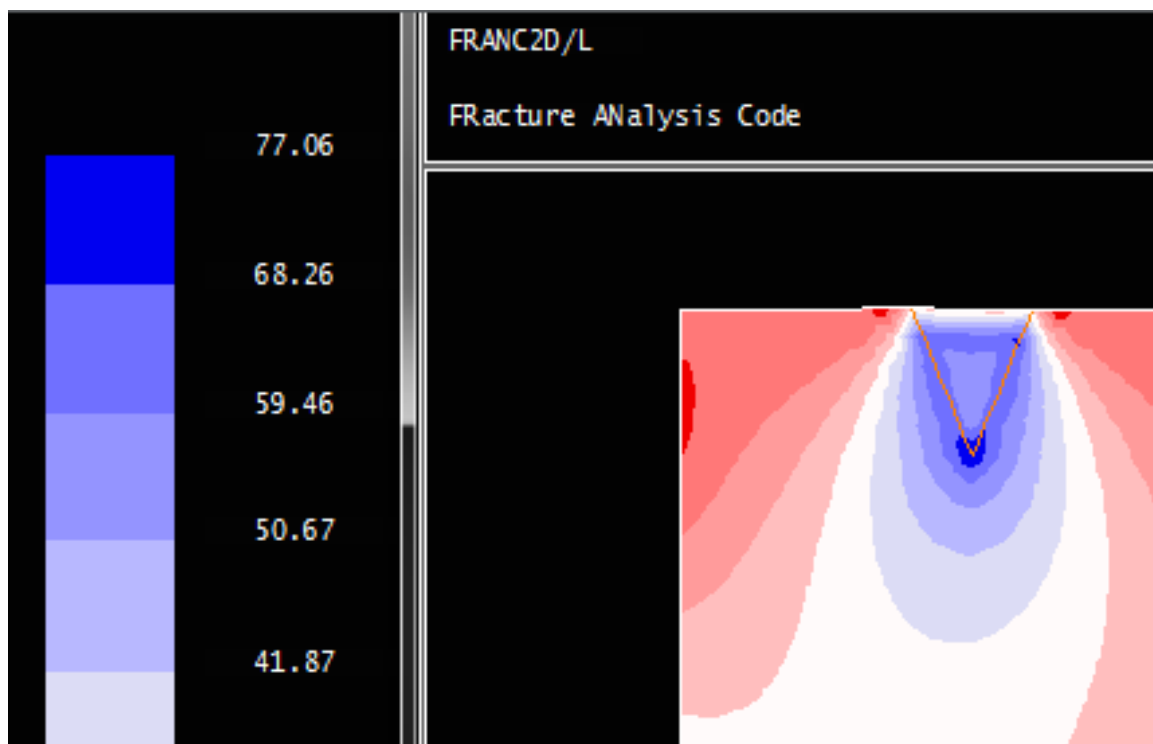


It was observed that the peak stress remained roughly constant (i.e. with negligible fluctuation) upto a minimum height of 6 inches, below which a sharp increase in peak stress was noted. Thus, it was concluded that a height of  $h/6$  was optimal for the triangular strip.

## Discussions

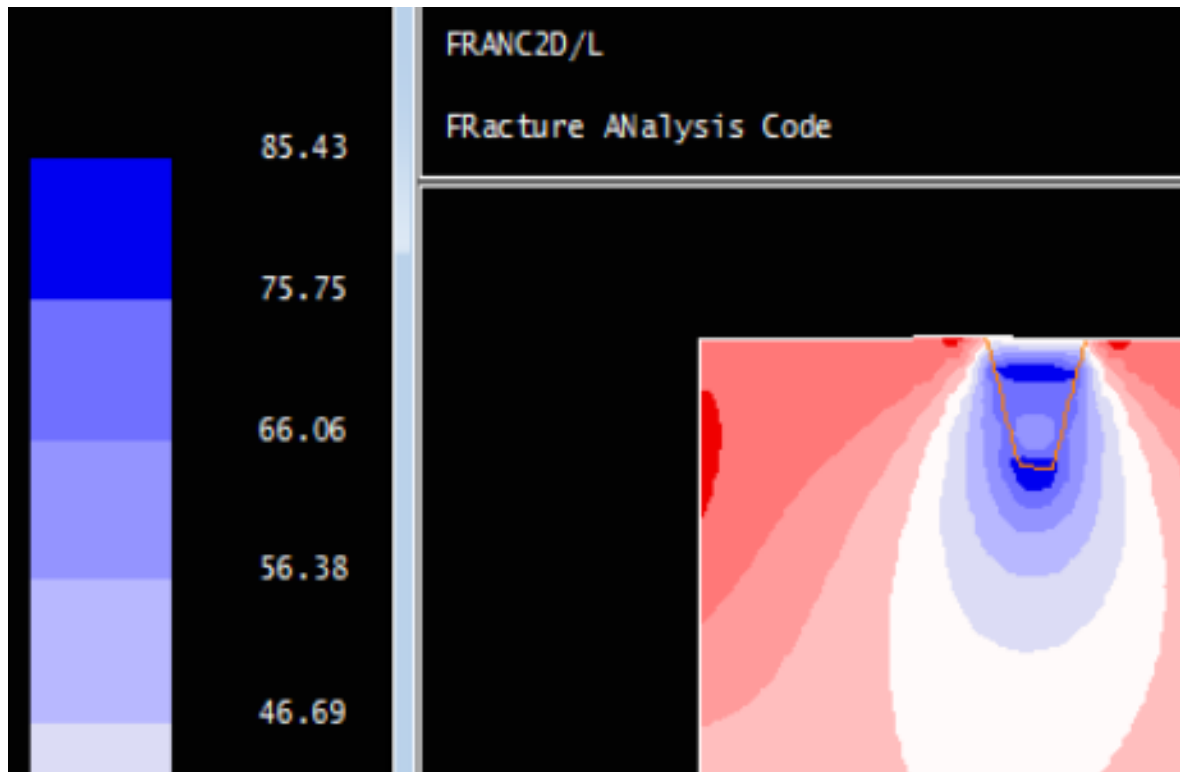
By maintaining a constant area and varying strip geometry, we managed to select efficient models from the peak stress observations. Once the trapezoidal and triangular models were proved to be worthy of being employed as strips, we attempted to optimize the strip area by reducing the height of the strips while keeping other dimensions constant. From the graphs plotted between peak stress and strip height values, it was observed that a strip height greater than  $h/8$  but lesser than  $h/4$  would be optimal in designing the bag. After carrying out simulations with a paper matrix, a height of  $h/6$  was observed to be optimal. However, a critical analysis of the trapezoidal and triangular strips at heights equalling a quarter of the full length provided us some insight into further scrutinizing the problem.

Illustrated below are the contour plots of triangular and trapezoidal strips (simulated with steel matrix), zoomed in to provide a better view of the area under maximum tension.



Triangular strip, strip height = 5inch





Trapezoidal strip, strip height = 5 inch

From the contour plots we may infer the following:

- 1) There is no marked difference in peak stress (only 10 psi) at such low strip lengths.
- 2) The area under maximum stress is much higher in case of the trapezoidal strip as when compared to the triangular strip.

Owing to a greater area under stress in case of the trapezoidal strip, the probability for failure becomes much greater. Additionally, the presence of more than one sharp corner (two as opposed to one in case of an isosceles triangular strip) implies a greater number of stress raisers in the strip, resulting in more plausible locations for failure to occur. Hence, keeping in mind the longevity of the bag; triangular strips might score over trapezoidal strips on all three fronts, namely; lower peak stress, lesser sites for stress raisers, and lower area subjected to maximum stress development.

## Conclusions

The ultimate objective of the project, i.e. to minimize peak stress and optimize stress distribution over the paper bag matrix was achieved as follows:

- A plain paper matrix of specified dimensions were taken and subjected to a simulated tensile test. With the load applied per handle being 50 pounds, the peak stress was observed to be **28.74 psi = 198 kPa**.
- When reinforced with parallel strips, the peak stress value came down to **78 kPa**.
- The down-up taper proved to be less effective than the parallel strip, with the peak stress being **118 kPa**.
- The trapezoidal up-down taper strip exhibited a peak stress value of **59 kPa**.
- The peak stress of the triangular strip was **44 kPa**.
- The peak stress of the height optimized strip, i.e. with height =  $h/6$  was approximately the same, i.e. **44 kPa**. An optimal strip height of 6 inches (under the given dimensions and constructs) exhibits good stress distribution and minimal peak stress, thereby economizing the process.

Thus, under the application of height optimized triangular strips, a reduction in peak stress of about 154 kPa was observed. Effective design and optimization lead to a percentage reduction in peak stress by about 77.78%.

## References

- 1) Plastic bag fact sheet, Sustainability Victoria, 9 November 2005
- 2) *Continuous jute fibre reinforced laminated paper composite and reinforcement-fibre free paper laminate*; B. B. Verma, Bulletin of Materials Sciences, Indian Academy of Sciences
- 3) CASCA: A simple 2-D Mesh Generator, Version 1.4; originally written by Paul Wawrzynek and Louis Martha, Cornell University
- 4) FRANC2D, A Two-Dimensional Crack Propagation Simulator, by Paul Wawrzynek and Louis Martha, Cornell University
- 5) *"On the in-plane elastic constraints of paper"* – Fibre Science and Technology 15 (1981), pp 257-270; Kalman Schulgasser